JPE 13-4-23

http://dx.doi.org/10.6113/JPE.2013.13.4.719

# A Novel Hybrid Active Power Filter with a High-Voltage Rank

Yan Li† and Gang Li*

*†School of Information Science and Engineering, Central South University, Hunan, China

**Abstract**

A novel hybrid active power filter (NHAPF) that can be adopted in high-voltage systems is proposed in this paper. The topological structure and filtering principle of the compensating system is provided and analyzed, respectively. Different controlling strategies are also presented to select the suitable strategy for the compensation system. Based on the selected strategy, the harmonic suppression function is used to analyze the influence of system parameters on the compensating system with MATLAB. Moreover, parameters in the injection branch are designed and analyzed. The performance of the proposed NHAPF in harmonic suppression and reactive power compensation is simulated with PSim. Thereafter, the overall control method is proposed. Simulation analysis and real experiments show that the proposed NHAPF exhibits good harmonic suppression and reactive power compensation. The proposed compensated system is based on the three-phase four-switch inverter, which is inexpensive, and the control method is verified for validity and effectiveness.

**Key words:** Harmonics suppression, reactive power compensation, active power filter, passive filter

## I. INTRODUCTION

Nonlinear loads and equipment in the consumer side, such as adjustable speed drives, arc furnaces, and controlled and uncontrolled rectifiers, cause problems in electrical systems [1]–[3] by polluting the power distribution system with harmonics. Utilities frequently encounter harmonic-related problems, such as harmonic interactions between utility and loads, reduced safety operating margins, reactive power, harmonic resonance, higher transformer and line losses, and capacitor failure caused by overloading [4]–[6].

Frequently used harmonic suppression equipment includes passive power filters (PPFs), active power filters (APFs), and hybrid APFs (HAPFs). PPF is used to eliminate the designated order of harmonic currents and compensate reactive power. However, PPFs have many disadvantages in practical applications, such as bulky and heavy devices and harmonic amplification caused by resonances [7]–[9]. APFs have been developed to overcome such problems [10]–[15]. Although APFs have good harmonic suppression performance, APFs are not suitable for high- or medium-voltage situations because they lack high-capacity semiconductor components. By contrast, HAPFs can eliminate harmonic currents in high- or medium-voltage situations [16]–[20]. Different HAPF topologies are composed of active and passive components in series and/or in parallel. These topologies aim to improve the compensation characteristics of PPFs and reduce the voltage and/or current ratings (costs) of APFs.

A novel hybrid APF (NHAPF) with a high-voltage rank is proposed in this paper. The active section of the NHAPF has insignificant fundamental voltages with such structure. This paper is organized as follows. Section II introduces the system structure of the NHAPF, as well as the filtering principle. Section III analyzes three controlling strategies. One of these strategies is selected to be the optimum controlling strategy. Section IV evaluates the NHAPF performance. The harmonic magnification characteristic and injection branch are analyzed in detail by using MATLAB. The harmonic suppression performance of NHAPF is analyzed under different conditions, such as the influence of the controlling magnification factor and grid inductor and PPF out of resonance. Section V analyzes the simulation and experiment results to verify the feasibility and validity of the proposed NHAPF and the controlling strategy. Finally, Section VI concludes.

Manuscript received Nov. 26, 2012; revised May 7, 2013
Recommended for publication by Associate Editor Sung-Yeul Park.
†Corresponding Author: liyanly@csu.edu.cn
Tel: +86-13467510867, Central South University
*School of Information Science and Engineering, Central South University, China

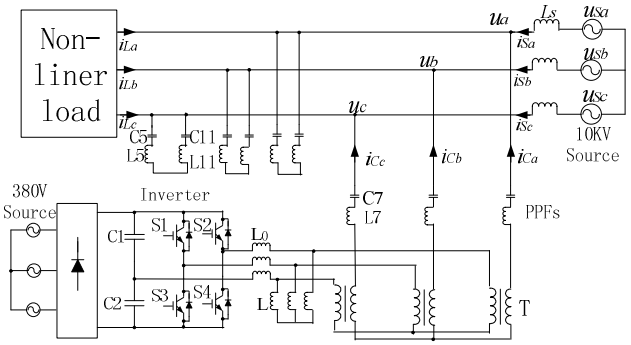


Fig.1. Topology structure of NHAPF.

## II. NHAPF STRUCTURE AND FILTERING PRINCIPLE

A simple-structured NHAPF that exhibits both harmonic suppression and reactive power compensation in a large power system is proposed in this paper. The NHAPF structure is shown in Fig. 1. The active section exhibits low fundamental voltages because the seventh PPF is connected to the active section. Thus, the requisite inverter capacity is also low. Parallel inductor L is connected to the second side of transformer T in parallel. Thus, the active section has a light lash, and the system can maintain stable when the system is power on or sudden change occurs in the grid voltage.

PPFs compose of the 5th, 7th, and 11th passive power filters. $L_0$ is the output filtering inductor for the active section. The APF connects the second side of the transformer after connecting to the output filter $L_0$ in series. Parallel inductor L is parallel to the second side of the transformer. The reactive power is compensated by the passive section, and the harmonic is suppressed by the active and passive sections. That is, the 5th and 11th harmonics are suppressed by the passive section, whereas the other harmonics are suppressed by the active section. The 7th PPF is the injection branch. The 7th PPF and inductor L share a grid voltage, thus enabling the active section to support low voltages and decreasing APF capacity. The compensation equipment can be used in a 10 KV grid.

The single-phase electrical model of the NHAPF in the harmonic field is shown in Fig. 2. The grid impedance is $Z_{Sh}$. The nonlinear load is considered the harmonic current source $I_{Lh}$. The active section is controlled as an ideal harmonic voltage source $U_C$. $I_{Sh}$, $I_{Ph}$, and $I_{Fh}$ are the grid, PPF, and injection branch currents, respectively. $Z_{Sh}$, $Z_{Ph}$, $Z_{7h}$, $Z_{Lh}$, and $Z_{L0h}$ are the impedance of the grid, 5th and 11th PPFs, 7th PPF, parallel inductor L, and output filter, inverter, and transformer, respectively. $Z_{Lh}$ and $Z_{L0h}$ are the equivalents in the first side of the transformer.

Based on Kirhoff's laws and Fig. 2, the following equations are derived:

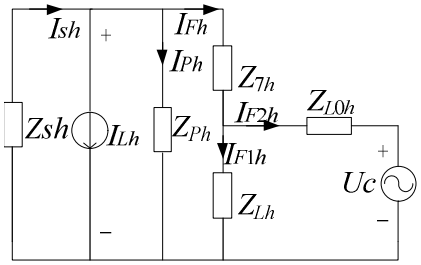


Fig. 2. Single-phase electrical model of the NHAPF in the harmonic field.

$$\begin{cases} I_{Sh} = I_{Ph} + I_{Fh} + I_{Lh} \\ I_{Sh}Z_{Sh} + I_{Ph}Z_{Ph} = 0 \\ I_{Sh}Z_{Sh} + I_{Fh}Z_{7h} + I_{F1h}Z_{Lh} = 0 \\ I_{Fh} = I_{F1h} + I_{F2h} \\ I_{F2h}Z_{L0h} + U_C = I_{F1h}Z_{Lh} \end{cases}. \quad (1)$$

Thereafter, it can be obtained as follows:

$$I_{Sh} = \frac{Z_h Z_{Ph} I_{Lh} - Z_{Ph} Z_{Lh} U_C}{Z_h Z_{Ph} + Z_h Z_{Sh} + Z_{Sh} Z_{Ph} (Z_{Lh} + Z_{L0h})}, \quad (2)$$

where $Z_h = Z_{7h}Z_{L0h} + Z_{7h}Z_{Lh} + Z_{Lh}Z_{L0h}$. Equation (2) shows that the grid harmonic current can be suppressed by controlling the voltage source $U_C$ of the inverter.

## III. CONTROLLING STRATEGY ANALYSIS

The working performance of the compensating equipment varies with different controlling strategies. The active section of the NHAPF can be controlled as a harmonic voltage source or current source. The active section is equivalent to the short circuit for the fundamental voltage if the active section is controlled as a harmonic voltage source. Even if the fundamental impedance of the parallel inductor $Z_{Lf}$ is small, the fundamental currents will still flow into the active section through the 7th PPF. However, if the equivalent fundamental impedance of the active section $Z_{L0f}$ is significantly greater than the fundamental impedance of the parallel inductor $Z_{Lf}$, the fundamental currents will flow into $Z_{Lf}$ through the 7th PPF. The harmonic impedance of the active section $Z_{L0h}$ increases with increasing $Z_{L0f}$. Thereafter, $Z_{L0h}$ shares more harmonic voltage, thus decreasing the harmonic suppression capability of the compensating equipment. That is, a contradiction exists between improving the harmonic suppression capability and decreasing the fundamental current in the active section if the active section is controlled as a harmonic voltage source.

If the active section of the NHAPF is controlled as a harmonic current source, the output current will contain insignificant values of the fundamental current component

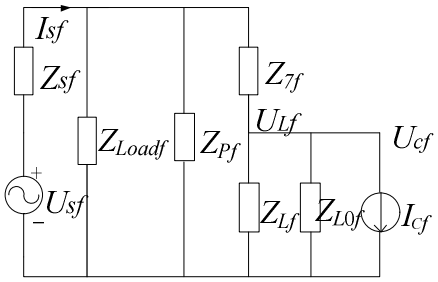


Fig. 3. Fundamental single-phase equivalent circuit that controls the active section as a harmonic current source.

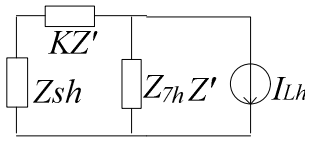


Fig. 4. Single-phase equivalent circuit of $f_1$.

$I_{Cf}$ because minimal $Z_{Lf}$ and $I_{Cf}$ will flow into the parallel inductor (Fig. 3).

Thus, the fundamental voltage on the active section is expressed as follows:

$$U_{Cf} = U_{Lf} \approx Z_{Lf} I_{Cf} \approx 0 \tag{3}$$

If the active section is controlled as the harmonic current source, $Z_{L0f}$ and its harmonic impedance will be small. The active section only has a small harmonic voltage, and the capacity of the active section is decreased. $Z_{L0f}$ will not affect the harmonic current from the active section, and the harmonic suppressing capability of the compensating equipment will not be affected.

Thus, the active section of the compensating equipment is controlled as the harmonic current source in this paper. Three controlling strategies are analyzed, and $Z_{L0h}$ is ignored because of its insignificant value. Equation (2) can be simplified as follows:

$$I_{Sh} = \frac{Z_{7h} Z_{Ph} I_{Lh} - Z_{Ph} U_C}{Z_{7h} Z_{Ph} + Z_{7h} Z_{Sh} + Z_{Sh} Z_{Ph}}. \tag{4}$$

The controlling strategy of the NHAPF can be designated by analyzing different controlling strategies:

(1) The active section is controlled as the grid harmonic current, $U_C = KI_{Sh}$, where $K$ is the controlling magnification factor. Thereafter, the harmonic suppressing function is expressed as follows:

$$f_1 = \frac{I_{Sh}}{I_{Lh}} = \frac{Z_{7h} Z_{Ph}}{Z_{7h} Z_{Ph} + Z_{7h} Z_{Sh} + Z_{Sh} Z_{Ph} + KZ_{Ph}}, \tag{5}$$

Let $Z' = \dfrac{Z_{Ph}}{Z_{Ph} + Z_{7h}}$,

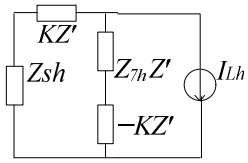


Fig. 5. Single-phase equivalent circuit of $f_2$.

$$f_1 = \frac{Z_{7h} Z'}{Z_{Sh} + (Z_{7h} + K) Z'}. \tag{6}$$

The single-phase equivalent circuit of the NHAPF (Fig. 4) is obtained according to Equation (6).

This controlling strategy can increase the adjustable harmonic impedance in the grid. The grid harmonic impedance can then be enlarged by controlling the APF, which allows the load harmonic currents to flow into the filtering branches instead of the grid.

(2) The active section is controlled as the load harmonic current, $U_C = KI_{Lh}$. Thereafter, the harmonic suppressing function is expressed as follows:

$$f_2 = \frac{I_{Sh}}{I_{Lh}} = \frac{Z_{7h} Z_{Ph} - KZ_{Ph}}{Z_{7h} Z_{Ph} + Z_{7h} Z_{Sh} + Z_{Sh} Z_{Ph}}, \tag{7}$$

Let $Z' = \dfrac{Z_{Ph}}{Z_{Ph} + Z_{7h}}$,

$$f_2 = \frac{(Z_{7h} - K) Z'}{Z_{7h} Z' + Z_{Sh}}. \tag{8}$$

The single-phase equivalent circuit of the NHAPF (Fig. 5) is obtained according to Equation (8).

The controlling strategy improves the harmonic impedance characteristic of the PPF and increases the grid harmonic impedance by controlling the APF, thus enhancing the filtering effect.

(3) The active section is controlled as the load harmonic current, $U_C = KI_{Fh}$. Thereafter, the harmonic suppressing function is expressed as follows:

$$f_3 = \frac{I_{Sh}}{I_{Lh}} = \frac{Z_{7h} Z_{Ph} + KZ_{Ph}}{Z_{7h} Z_{Ph} + Z_{7h} Z_{Sh} + Z_{Sh} Z_{Ph} + K(Z_{Sh} + Z_{Ph})}, \tag{9}$$

Let $Z'' = \dfrac{Z_{Ph} Z_{7h} + KZ_{Ph}}{Z_{Ph} + Z_{7h} + K}$,

$$f_3 = \frac{Z''}{Z_{Sh} + Z''}. \tag{10}$$

The single-phase equivalent circuit of the NHAPF (Fig. 6) is obtained according to Equation (10) .

The controlling strategy improves the harmonic impedance characteristic of the PPF by controlling the APF. The load harmonic currents can then be eliminated theoretically. However, difficulty arises when the grid contains high harmonic voltages.

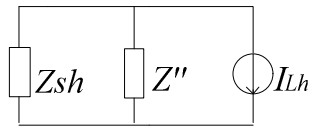


Fig. 6. Single-phase equivalent circuit of $f_3$.

TABLE I

SIMULATION PARAMETERS OF NHAPF

| Filters | Capacitor/μF | Inductor/mH |
|---|---|---|
| The 5th PPF | 8.6 | 48.585 |
| The 11th PPF | 3.69 | 23.423 |
| Output filter | / | 0.5 |
| Parallel inductor | / | 8 |
| The 7th PPF | 2.8 | 73.56 |

## IV. NHAPF PERFORMANCE

### A. Harmonic Magnification Characteristic

The active section improves the PPF performance even though the NHAPF contains capacitors and inductors. The levels of improvement vary with different controlling strategies. The harmonic current magnification factor is defined as the ratio of the grid harmonic current and load harmonic current. Three harmonic current magnification factors that correspond to the three controlling strategies are obtained according to Equation (2).

(1) If the active section is controlled as $U_C = KI_{Sh}$, the harmonic current magnification factor is expressed as follows:

$$f_{I_{Sh}} = \frac{Z_h Z_{Ph}}{Z_h Z_{Ph} + Z_h Z_{Sh} + KZ_{Ph} Z_{Lh} + Z_{Sh} Z_{Ph} (Z_{Lh} + Z_{L0h})} . \quad (11)$$

(2) If the active section is controlled as $U_C = KI_{Lh}$, the harmonic current magnification factor is defined as the following:

$$f_{I_{Lh}} = \frac{Z_h Z_{Ph} - KZ_{Ph} Z_{Lh}}{Z_h Z_{Ph} + Z_h Z_{Sh} + Z_{Sh} Z_{Ph} (Z_{Lh} + Z_{L0h})} . \quad (12)$$

(3) If the active section is controlled as $U_C = KI_{Fh}$, the harmonic current magnification factor is expressed as follows:

$$f_{I_{Fh}} = \frac{Z_h Z_{Ph} - KZ_{Ph} Z_{Lh}}{Z_h Z_{Ph} + Z_h Z_{Sh} + KZ_{Sh} Z_{Ph} (Z_{Lh} + Z_{L0h})} . \quad (13)$$

Equations (11), (12), and (13) are simulated by using MATLAB. The simulation parameters of NHAPF are shown in Table 1.

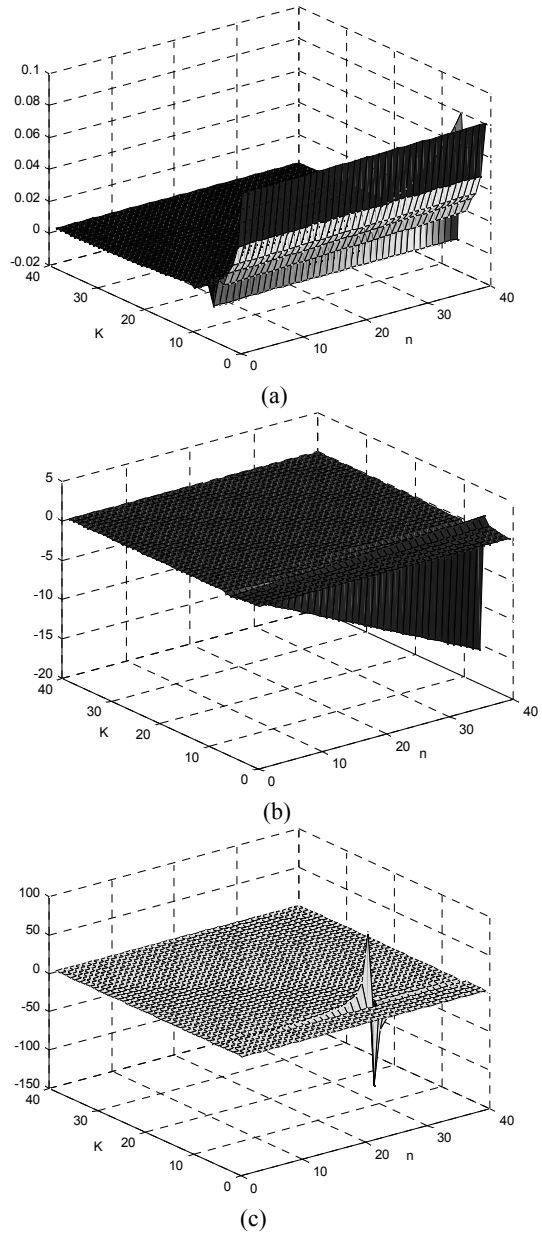


Fig. 7. Simulation results: (a) $U_C = KI_{Sh}$; (b) $U_C = KI_{Lh}$; (c) $U_C = KI_{Fh}$.

The simulation results are shown in Fig. 7. Coordinates *Z*, *X*, and *Y* represent the magnification factor, harmonic order *n*, and controlling magnification factor *K*, respectively.

The probability of resonance caused by the PPF and the grid can be decreased when the active section is controlled as $U_C = KI_{Sh}$ (Fig. 7). The other two controlling strategies can cause resonance in the system.

### B. Injection Branch Analysis

The selection of the 7th PPF as the injection branch is first analyzed with the harmonic current magnification factor. Equation (11) is selected as the harmonic current

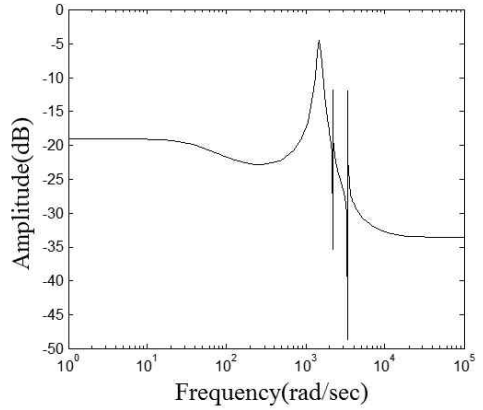


Fig. 8. Harmonic suppression performance when the injection branch is the fifth PPF.

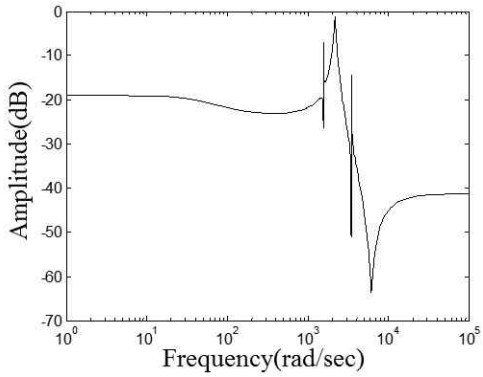


Fig. 9. Harmonic suppression performance when the injection branch is the seventh PPF.

magnification factor according to the above analysis. The 5th, 7th, and 11th PPFs act as the injection branch, and the corresponding harmonic suppression functions are simulated. The controlling magnification factor is set to 10.

When the injection branch is the 5th PPF, $Z_{Ph}=\frac{Z_{7h}Z_{11h}}{Z_{7h}+Z_{11h}}$. $Z_{5h}$, $Z_{7h}$, and $Z_{11h}$ denote the equivalent harmonic impedances of the 5th , 7th, and 11th PPFs, respectively. The baud corresponding to the harmonic current magnification factor is shown in Fig. 8.

When the injection branch is the seventh PPF, $Z_{Ph}=\frac{Z_{5h}Z_{11h}}{Z_{5h}+Z_{11h}}$, $Z_{2h}=Z_{7h}$. The baud corresponding to the harmonic current magnification factor is shown in Fig. 9.

When the injection branch is the 11th PPF, $Z_{Ph}=\frac{Z_{7h}Z_{5h}}{Z_{7h}+Z_{5h}}$. The baud corresponding to the harmonic current magnification factor is shown in Fig. 10.

The simulation results show that all order harmonics are suppressed well, particularly the high-order harmonics, when the injection branch is the 5th or 7th PPF. The 7th harmonic is magnified when the injection branch is the 11th PPF. Considering that the 7th harmonic component is lower than

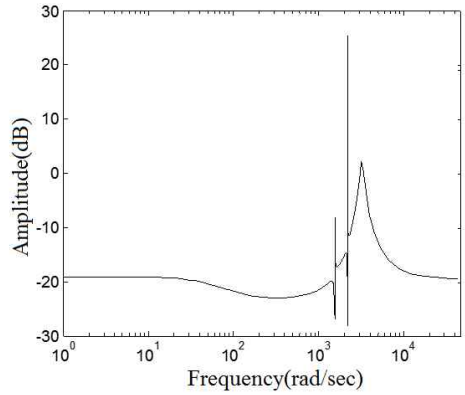


Fig. 10. Harmonic suppression performance when the injection branch is the seventh PPF.

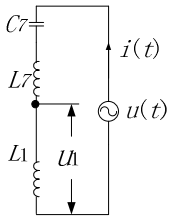


Fig. 11. Single-phase equivalent circuit corresponding to the capacitive reactive compensating branch.

the 5th harmonic component, the 7th PPF is selected as the injection branch. Comparisons of the NHAPF structure with the injection branch by using the 5th PPF show that the NHAPF structure requires fewer capacities than the APF. In the NHAPF structure, the 5th and 11th harmonic currents are suppressed by the PPFs, and the 7th and higher harmonic currents are suppressed by the APF.

The single-phase equivalent circuit corresponding to the capacitive reactive compensating branch that uses the 7th PPF is shown in Fig. 11 when the grid voltages show an abnormal phenomenon.

In Fig. 11, $L_1$ is the equivalent first-side inductor of parallel inductor L connected to the second side of the transformer. $u(t)$ is the abnormal voltage (e.g., voltage drop). If the grid voltage decreases, the decreasing voltage has the same frequency and opposite phase as the grid voltage. The frequency and phase of the decreasing voltage is added to the grid voltage. The decreasing voltage can be expressed as follows:

$$u(t)=-A\sqrt{2}U\sin(\omega_0 t), \tag{14}$$

where $A$ denotes the level of voltage drop in the grid. $U$ and $\omega_0$ indicate the effective value and frequency of the grid voltage, respectively. Based on Fig. 11, the following equation can be obtained:

$$(L_i+L_1)\frac{di(t)}{dt}+\frac{1}{C_i}\int i(t)dt=u(t). \tag{15}$$

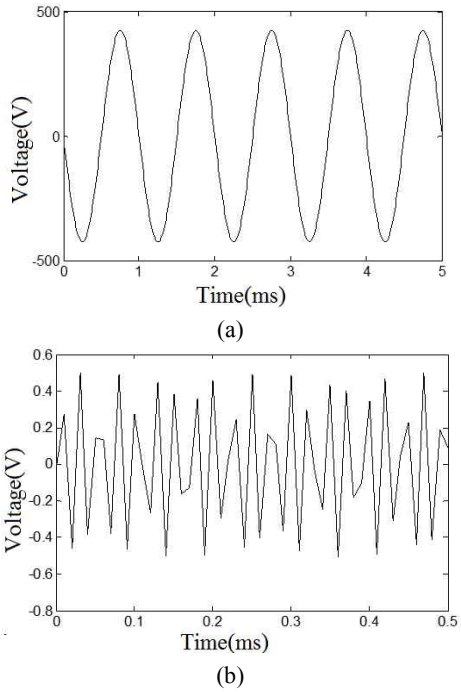


Fig. 12. Voltage of the fundamental split-flow branch with voltage drop: (a) grid voltage drop and (b) voltage on the fundamental split-flow branch.

By setting the state variables as $x_1 = i(t)$ and $x_2 = \frac{1}{C_i}\int i(t)dt$, the output is $y_H = u_1 = L_1 \frac{di(t)}{dt}$. The state equation can be obtained as follows:

$$\begin{bmatrix} \dot{x}_1 \\ \dot{x}_2 \end{bmatrix} = \begin{bmatrix} 0 & -\frac{1}{L_i + L_1} \\ \frac{1}{C_i} & 0 \end{bmatrix} \begin{bmatrix} x_1 \\ x_2 \end{bmatrix} + \begin{bmatrix} \frac{1}{L_i + L_1} \\ 0 \end{bmatrix} u(t), \quad (16)$$

$$y_H = \begin{bmatrix} 0 & \frac{-L_1}{L_i + L_1} \end{bmatrix} \begin{bmatrix} x_1 \\ x_2 \end{bmatrix} + \begin{bmatrix} \frac{L_1}{L_i + L_1} \end{bmatrix} u(t). \quad (17)$$

By setting $\omega_{H1} = \sqrt{\frac{1}{C_i(L_i + L_1)}}$, the system zero state response is defined as follows:

$$y_H(s) = \frac{\omega_{H1}^3 C_i L_1 A\sqrt{2} U \omega_0}{\omega_{H1}^2 - \omega_0^2} \frac{\omega_{H1}}{s^2 + \omega_{H1}^2} + \left(\frac{\omega_{H1}^4 C_i L_1 A\sqrt{2} U}{\omega_0^2 - \omega_{H1}^2} - \omega_{H1}^2 C_1 L_1 A\sqrt{2} U\right) \frac{\omega_0}{s^2 + \omega_0^2}, \quad (18)$$

The corresponding output response in the time domain is expressed as follows:

$$y_H(t) = f_1 \sin(\omega_1 t) + f_2 \sin(\omega_0 t), \quad (19)$$

where $f_{H1} = \frac{\omega_{H1}^3 C_i L_1 A\sqrt{2} U \omega_0}{\omega_{H1}^2 - \omega_0^2}$, and $f_{H2} = \frac{\omega_{H1}^4 C_i L_1 A\sqrt{2} U}{\omega_0^2 - \omega_{H1}^2} - \omega_{H1}^2 C_1 L_1 A\sqrt{2} U$.

When a voltage drop occurs in the grid, inductor $L_1$ bears the fundamental voltage with amplitude $f_{H2}$ and the harmonic voltage with amplitude $f_{H1}$ frequency $\omega_{H1}$. In this paper, the grid drop voltage is set as follows:

$$u(t) = -300\sqrt{2} \sin(2 * 50 * \pi * t). \quad (20)$$

The fundamental split-flow branch has an insignificant voltage when the grid voltage shows sudden changes in selecting the 7th PPF as the injection branch (Fig. 12). This result means that the active section has an insignificantlittle voltage.

### C. The harmonic suppressing performance of NHAPF

At first, the harmonic suppressing function is defined as the specific value between the grid harmonic current $I_{Sh}$ and the load harmonic current $I_{Lh}$ without the grid harmonic voltage. The harmonic suppressing function indicates the suppressing harmonic capability of the compensating equipment. The harmonic suppressing function is the equation (11) for NHAPF with $U_C = KI_{Sh}$.

The stable compensating characteristic of NHAPF is analyzed with the harmonic suppressing function. If PPFs just are put into the grid in the NHAPF, then the harmonic suppressing function is:

$$f_{PPF} = \frac{Z'_{Ph}}{Z'_{Ph} + Z_{Sh}} \quad (21)$$

Where, $Z'_{Ph} = \frac{Z_{Ph} Z_{7h}}{Z_{Ph} + Z_{7h}}$. The harmonic suppressing performance of NHAPF is analyzed from some aspects such as the controlling magnification factor, the grid impedance and the out of resonance for PPF.

*1) The influence of the controlling magnification factor:* Amplitude and frequency characteristic curves of harmonic suppressing functions with different controlling magnification factors putting PPFs and putting NHAPF respectively into the grid are given in Fig.13. The system inductor is $L_S$=0.5mH.

From the Fig.13 (a) it can be found out that the compensating equipment just putting PPFs acts on fixed or high frequency harmonic currents. In the case, the controlling magnification $K$ equals 0. The grid low frequency harmonic currents are hardly suppressed. There are three obvious resonance points in the system. It is easy to have resonance for the system when the grid contains corresponding high harmonic voltages. When the active section is put into the grid, amplitudes in all frequencies decrease (Fig. 13(b)). The harmonic suppressing effect is also significantly improved,

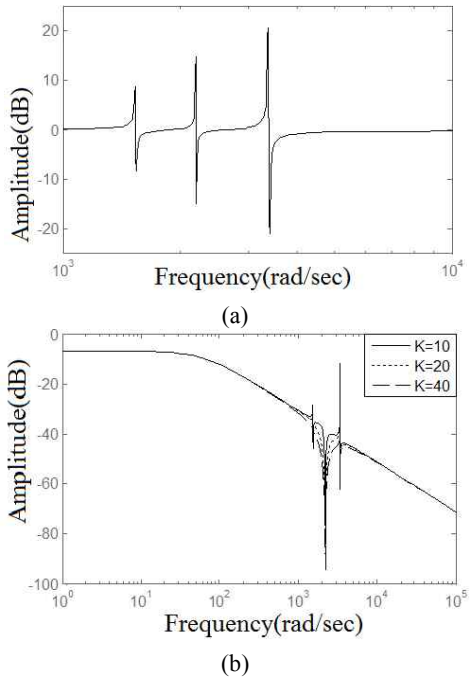


Fig. 13. Influence of the controlling magnification factor on the harmonic suppression function: (a) placing of PPFs into the grid; (b) placing of NHAPF into the grid.

and the harmonic current in the grid is insignificant. The amplitude and frequency characteristic curves of the harmonic suppressing functions with $K$ = 10, 20, and 40 are shown in Fig. 13(b). A higher $K$ value corresponds to a better harmonic suppressing effect. However, the value of $K$ does not need to be very high. If the value of $K$ is set excessively high, the system becomes unstable.

*2) Influence of the grid inductor:* The amplitude and frequency characteristic curves of the harmonic suppressing functions with different grid inductors that place PPF and NHAPF into the grid are shown in Fig. 14. The controlling magnification factor $K$ is set to 10. Let the inductor $L_S$ be equal to 0.5, 1, and 2 mH.

The resonance points move to a low frequency with increasing $L_S$ and when placing PPFs (Fig. 14(a)). A higher $L_S$ value corresponds to a better suppressing effect. After placing the active section, the places of the resonance points with different $L_S$ values are not affected. Moreover, the amplitude and frequency characteristic curves of the harmonic suppressing functions before the last resonance point show insignificant changes. The active section just acts in the frequency range, and the change in $L_S$ has insignificant influence on APF. A higher $L_S$ value corresponds to a better suppressing effect in the frequency range after the last resonance point because PPF is affected by $L_S$. That is, NHAPF has a good suppressing effect on all frequency harmonic currents.

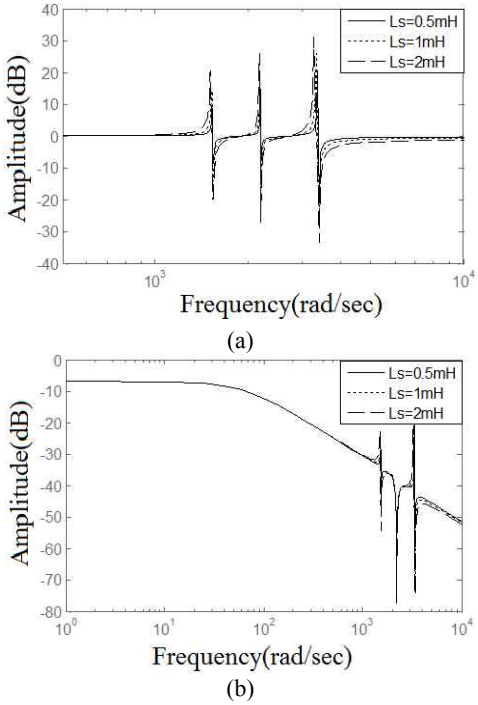


Fig. 14. Influence of the grid inductor on the harmonic suppression function: (a) placing of PPFs into the grid; (b) placing of NHAPF into the grid.

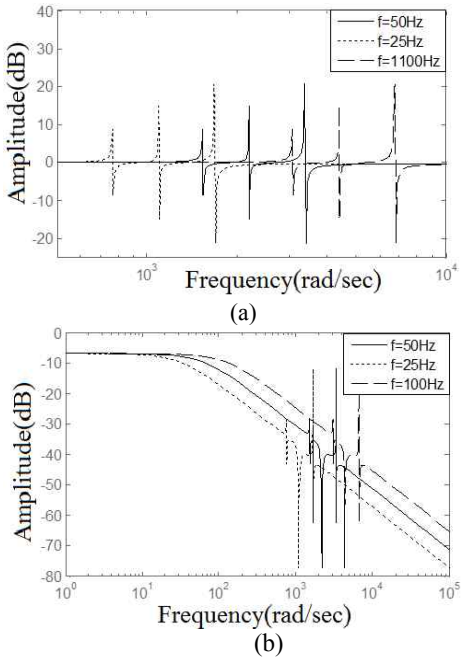


Fig. 15. Influence of out of resonance for PPFs: (a) placing PPF into the grid; (b) placing NHAPF into the grid.

*3) Influence of out of resonance for PPFs:* Given the influence of the external world or small manufacturing errors, a PPF may not resonate at its resonance point. This phenomenon is called out of resonance. When the fundamental frequency is out of resonance by ±50%, the resonance frequencies of the 5th, 7th, and 11th PPFs are 125/500, 175/700, and 275/1100 Hz, respectively.

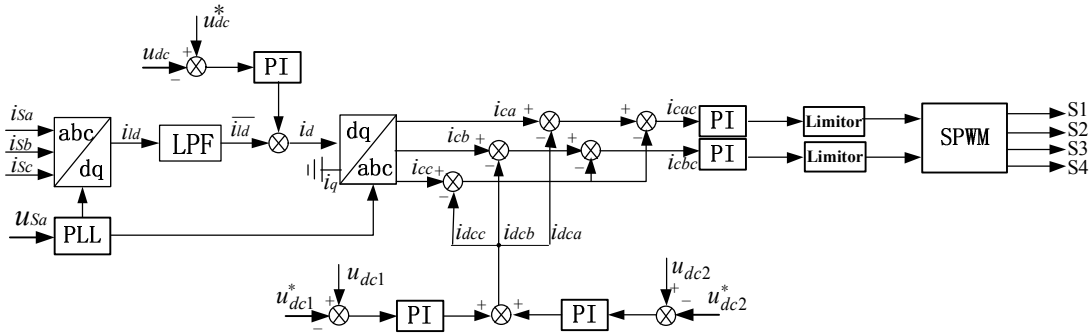


Fig. 16. Overall control diagram.

Three curves show the same changes, thus causing a translation movement with changing frequencies (Fig. 15). The three curves have the same harmonic suppressing effect. The harmonic suppressing function is lower than 0 dB in all frequencies under the out of resonance condition for NHAPF. This result indicates that the NHAPF has good harmonic suppressing effects.

## V. Overall Control

The overall control diagram of the NHAPF is shown in Fig. 16.

The general voltage on the DC-link and the voltages on DC-link capacitors C1 and C2 are controlled to balance the two capacitors and maintain the stability of the whole DC-link voltage in the overall control strategy. The general voltage on the DC-link is controlled and combined with the reference current method of ip-iq. $u_{dc}^{*}$ is the given voltage for the general voltage on the DC-link $u_{dc}$. The error between the DC-link is caused by the Proportion Integration (PI) regulator. A regulating signal is then obtained and is added to the direct component of the instant active current. The voltages on DC-link capacitors C1 and C2 are controlled by two PI regulators. Three currents, namely, $i_{dca}$, $i_{dcb}$, and $i_{dcc}$ are then obtained. These three currents are subtracted by three reference currents, namely, $i_{ca}$, $i_{cb}$, and $i_{cc}$ from the ip-ip method. Currents $i_{cac}$ and $i_{cbc}$ are the final reference currents. These two currents are obtained through two PI regulators and limiters. The triggering signals are gained after Pulse-width Modulation (PWM).

## VI. Simulation and Experimental Results

The simulation parameters of the NHAPF are obtained by PSim simulation (Table 1). The voltage source is 35 kV with 50 Hz. The capacitance of each DC-link capacitor is 10000 $\mu$F. The gate of each PI regulator is 10, and the time constant is 0.1. The grid current curves and corresponding spectra are shown in Fig. 17 before placing the NHAPF. The grid currents distort significantly, and the power factor is low at only 0.87.

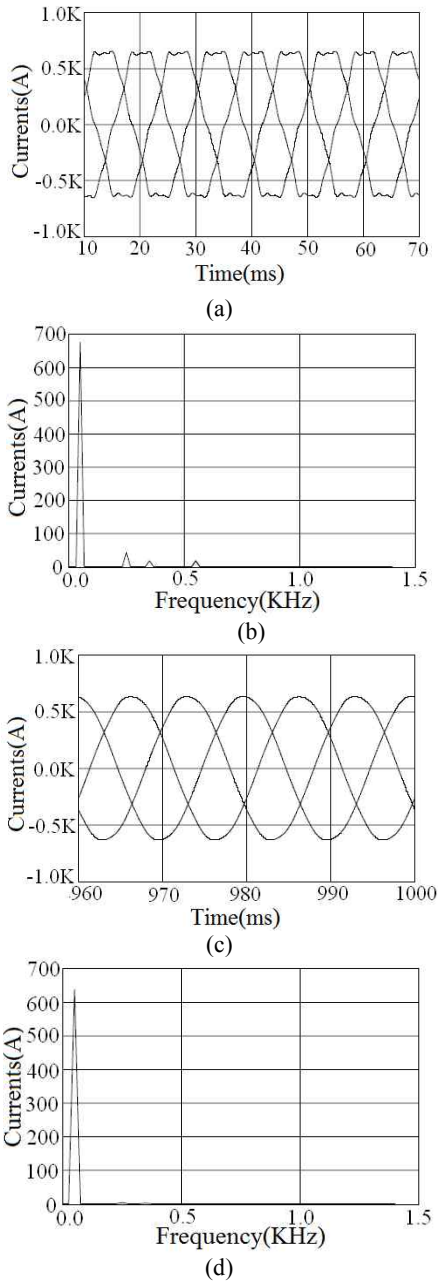


Fig. 17. Simulation results: (a) grid currents before placing the NHAPF; (b) spectra of the grid currents before placing the NHAPF; (c) grid currents after placing the NHAPF; (d) spectra of the grid currents after placing the NHAPF.

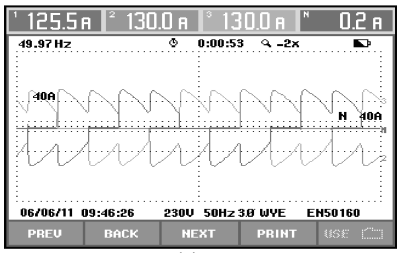


(a)

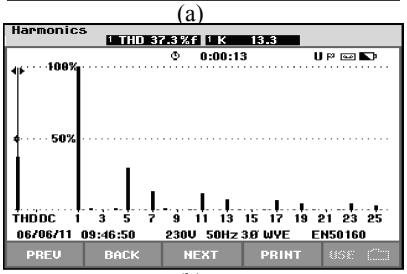


(b)

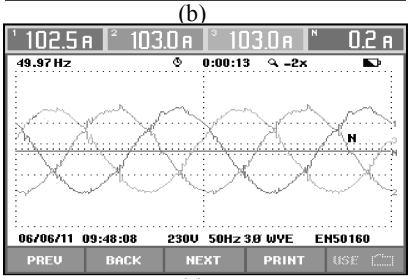


(c)

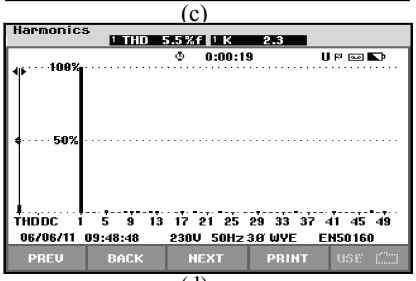


(d)

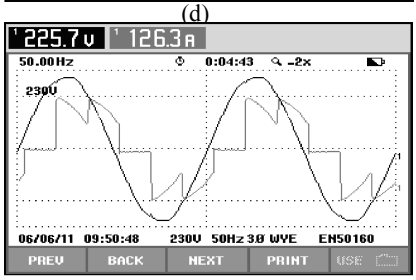


(e)

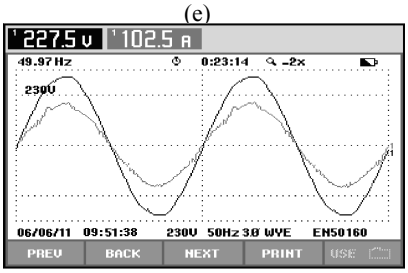


(f)

Fig. 18. Experimental results: (a) grid currents before placing the NHAPF; (b) spectra of the grid currents before placing the NHAPF; (c) grid currents after placing the NHAPF; (d) spectra of the grid currents after placing the NHAPF; (e) grid voltage and current before placing the NHAPF; (f) grid voltage and current after placing the NHAPF.

The simulation results show that the distortion of the grid current is decreased and that the main order harmonic currents are decreased after placing the NHAPF. The power factor is improved to 0.95.

The experimental equipment of the NHAPF is established in the laboratory with a voltage source of 380 V. The load is a three-phase rectifying device. The experimental curves are shown in Fig. 18. Heavy distortion can be observed in the grid currents, and Total Harmonic Distortion (THD) is 37.3% before placing the NHAPF. The phase angle error between the grid voltage and current is large. The grid currents are improved, and THD is 5.5% after placing the NHAPF. The phase angle error between the grid voltage and current is greatly reduced, and the power factor is improved to 0.95.

## VII. CONCLUSIONS

An NHAPF with a high-voltage rank is proposed in this paper. The NHAPF equipment has several characteristics. A small inductor is placed parallel to the second side of the transformer. The APF that is connected to the output filter in a series connects the second side of the transformer and the small inductor in parallel. Thereafter, the APFs connect the seventh PPF with the grid. This structure can enable the APF to have a small voltage, which decreases APF capacity and improves equipment reliability. The principle of the NHAPF is then presented, and different performance parameters are analyzed and simulated. The overall control method is proposed corresponding to the proposed compensated system based on the three-phase four-switch inverter, and experimental equipment is established for the experiments. The simulation and experimental results show that the proposed equipment, which is inexpensive, is feasible and exhibits good performance in suppressing the harmonic and reactive power.

## REFERENCES

[1] F. Blaabjerg, R. Teodorescu, M. Liserre, and A. V. Timbus, "Overview of control and grid synchronization for distributed power generation systems," *IEEE Trans. Ind. Electron.,* Vol. 53, No. 5, pp. 1398-1409, Oct. 2006.

[2] B. Singh, K. Al-Haddad, and A. Chandra, "A review of active filters for power quality improvement," *IEEE Trans. Ind. Electron.*, Vol. 46, No. 5, pp. 960-971, Oct. 1999.

[3] B. R. Lin and C. H. Huang, "Implementation of a three-phase capacitor clamped active power filter under unbalanced condition," *IEEE Trans.Ind. Electron*., Vol. 53, No. 5, pp. 1621-1630, Oct. 2006.

[4] T. D. Kefalas and A. G. Kladas, "Harmonic impact on distribution transformer no-load loss," *IEEE Trans. Ind. Electron.*, Vol. 57, No. 1, pp. 193-200, Jan. 2010.

[5] S. Rahmani, N. Mendalek, and K. AI-Haddad, "Experimental design of a nonlinear control technique for three-phase shunt active power filter," *IEEE Trans. Ind. Electron*., Vol. 57, No. 10, pp. 3364-3375, Oct. 2010.

[6] R. S. Herrera, P. Salmerón, and H. Kim, "Instantaneous

reactive power theory applied to active power filter compensation: Different approaches, assessment, and experimental results," *IEEE Trans. Ind. Electron*., Vol. 55, No. 1, pp. 184-196, Jan. 2008.
[7] J. C. Das, "Passive filters-potentialities and limitations," *IEEE Trans. Ind. Appl.*, Vol. 40, No. 1, pp. 232-241, Jan. 2004.
[8] M. Wien, H. Schwarz, and T. Oelbaum, "Performance Analysis of SVC," *IEEE Trans. Circuits Syst. Video Technol.*, Vol. 17, No. 9, pp. 1194 - 1203, Sep. 2007
[9] A. Luo, Z. K. Shuai, Z. J. Shen, W. J. Zhu, and X. Y. Xu, "Design considerations for maintaining dc-side voltage of hybrid active power filter with injection circuit," *IEEE Trans. Power Electron.*, Vol. 24, No. 1, pp. 75-84, Jan. 2009.
[10] E. E. EL-Kholy, A. EL-Sabbe, A. El-Hefnawy, and H. M. Mharous, "Three-phase active power filter based on current controlled voltage source inverter," *International journal of Electrical Power and Energy Systems*, Vol. 28, No. 8, pp. 537-547, Oct. 2006.
[11] S. A. Gonzalez, R. G. Retegui, and M. Benedetti, "Harmonic computation technique suitable for active power filters," *IEEE Trans. Ind. Electron.*, Vol. 54, No. 5, pp. 2791-2796, Oct. 2007.
[12] J.-C. Wu, H.-L. Jou, and Y.-T. Feng, "Novel circuit topology for three-phase active power filter," *IEEE Trans. Power Del*., Vol. 22, No. 1, pp. 444-449. Jan.2007.
[13] K. K. Shyu, M. J. Yang, Y. M. Chen, and Y. F. Lin, "Model reference adaptive control design for a shunt active-power-filter system," *IEEE Trans. Ind. Electron*., Vol. 55, Vol. 1, pp. 97-106, Jan. 2008.
[14] J. Kim, J. Hong, and K. Nam, "A current distortion compensation scheme for four-switch inverters," *IEEE Trans. Power Electron.*, Vol. 24, No. 4, pp. 1032-1040, Apr. 2009.
[15] S. Rahmani, A. Hamadi, N. Mendalek, and K. Haddad, "A new control technique for three-phase shunt hybrid power filter," *IEEE Trans. Ind. Electron.*, Vol. 56, No. 8, pp. 2904-2915, Aug. 2009.
[16] H.-L. Jou, J.-C. Wu, K.-D. Wu, M.-S. Huang, C-A. Lin, "A hybrid compensation system comprising hybrid power filter and AC power capacitor," *International Journal of Electrical Power and Energy Systems*, Vol. 28, No. 7, pp. 448-458, Sep. 2006.
[17] A. Luo, C. Tang, Z. K. Shuai, W. Zhao, F. Rong, and K. Zhou, "A novel three-phase hybrid active power filter with a series resonance circuit tuned at the fundamental frequency," *IEEE Trans. Ind. Electron.,* Vol. 56, No.7, pp. 2341-2440, Jul. 2009.
[18] A. Luo, Z. Shuai, W. Zhu, and Z. J. Shen, "Combined system for harmonic suppression and reactive power compensation," *IEEE Trans. Ind. Electron.,* Vol. 56, No. 2, pp. 418-428, Feb. 2009.
[19] V. F. Corasaniti, M. B. Barbieri, P. L. Arnera, and M. I. Valla, "Hybrid active filter for reactive and harmonics compensation in a distribution network," *IEEE Trans. Ind. Electron.*, Vol. 56, No. 3, pp. 670-677, Mar. 2009.
[20] P. Salmer´on and S. P. Litr´an. "A control strategy for hybrid power filter to compensate four-wires three-phase systems," *IEEE Trans. Power. Electron.,* Vol. 25, No. 7, pp. 1923-1931, Jul. 2010.

**Yan Li** was born in Guangxi, China in 1976. She received her BS, MS, and PhD in automatic, disaster prevention, and mitigation engineering and pattern recognition and intelligent system from Central South University, Changsha, China in 1999, 2003, and 2007, respectively. She also performed research works in the electrical engineering post-doctoral research station of Hunan University. She has been working as a teacher in the School of Science Information and Engineering of Central South University, Changsha, China since 2003. Her current research interests include power quality, power control, and fault diagnosis of electrical machines. She is currently finishing her post-doctoral studies.

**Gang Li** was born in Chongqing, China in 1977. He received his BS and MS in automatic and computer science from Central South University, Changsha, China, in 1999 and 2005, respectively. He has been a doctoral student in Central South University, China since 2008. He has been working as a teacher in the School of Science Information and Engineering, Central South University, Changsha, China since 1999. His current research interests include power electronics and control.